Geochemistry and Radioactivity of Abu Thora Formation Southwest Sinai, Egypt

Adel H. El Afandy, Ahmed E. Shata and Khaled Abd El Halim

Nuclear Materials Authority

ABSTRACT

The Abu Thora Formation consists mainly of sandstones, siltstones and shales deposited in a terrestrial foreland basin in active continental margin. Modal abundances of quartz, feldspar and rock fragments show that these sandstones have quartz arenite, sublithic and lithic arenite composition. The provenance of quartz grain revealed the mixed plutonic and low grade metamorphic parent rocks. The observed heavy minerals include monazite, apatite, zircon, rutile and sphene. These heavy grains and mica also occur as tiny inclusions in quartz grains of plutonic provenance. The studied sandstones, siltstones and shales are enriched in Co, Ni, Zr, V, Sr, Nb and U in comparison with the Upper Continental Crust (UCC), while, they are depleted in Al_2O_3, Na_2O, K_2O, Cr, Th, Rb and Ba. Abu Thora Formation deposited as first cycle of deposition. The chemical index of alteration (CIA) values indicate that the source area are strongly affected by significant chemical weathering. The recycling could have produced the interbedded claystones and siltstones. Abu Thora Formation shows a positive disequilibrium where the chemical U is higher than the radiometric ones. The anomalous U content (up to 72 ppm Uc) in Abu Thora Formation is controlled mainly by the presence of

U-bearing detrital grains. Enrichment of U and other mobile elements have been remobilized from the Precambrian granitoid source rocks and the underlying radioactive Um Bogma Formation. The leachable uranium hosted in the interbeded mudstones and siltstones is captured by the dominant iron oxides, clay mineral and organic matter in these lithofacies.

INTRODUCTION

The geochemical composition of sandstones is affected and controlled by various factors such as source rocks, weathering processes, transportation and diagenesis. Tectonsim has been suggested to control sedimentary composition (Pettijhon et al., 1972; Blatt et al., 1980). The textural characteristics of sandstone units are the product of weathering, transportation and sedimentary processes, while the compositions also depends on the primary chemical composition of the source rock area and the tectonic setting of the depositional basins (Bhatia and crook, 1986). McLennan (1985) noted that concentration of major, trace and rare earth elements (REE) of sediments are well suited to constrain provenance and source rock composition.

Abu Thora Formation is the upper clastics unit overlying the famous mineralized Um Bogma Formation in east Abu Zenima area, southwest Sinai. The sequence of Abu Thora was regarded as Ataqa Series (Kostandi, 1959), Ataqa Group (Soliman and Abu El Fetouh, 1969), Ataqa Formation (Said, 1971) or Abu Zarab Formation (El-Shazly et al., 1974) in the previous literature. The Ataqa Series or Ataqa Formation

was used to describe different sections mainly of Upper Carboniferous to Permian age. Weissbrod (1980) was the first author assigned the term Abu Thora Formation to the rock unit equivalent to the three formations; El Hashash, Magharet El Maih and Abu Zarab formations of Soliman and Abu El Fetouh (1969). He studied the well developed exposures of Abu Thora Formation at Wadi Thora (type locality), east Abu Zenima, southwest Sinai. Kora (1984) identified 32 species of spores and assigned the Upper Visean age to Abu Thora Formation. Many authors were studied the Abu Thora Formation among of them are: Omara and Schult (1965); Weissbrod (1969); Soliman and Abu El Fetouh, (1969); Kora (1984); Bhattacharyya and Dun (1986); El Agami, (1996); El Kelani et al. (1999); El Aassy et al. (2006) and El Sawey, (2008). But no one of them dealt with the detailed radioactivity and geochemistry of this formation.

Uranium mineralization in southwest Sinai has been early discovered in Um Bogma Formation (El Aassy et al., 1986; Hussein et al., 1992; El Agami, 1996). The priority of Abu Thora Formation for hosting U mineralization is attributed to its stratigraphic position in Paleozoic succession which unconformably overlying the crystalline basement rocks of the Arabo-Nubian Shield. The latter are considered the source of radioactive mineralization in the study area.

The present work is considered the first study which deals with the geochemical and radioactive characteristics of Abu Thora Formation. The study area is located at southwest Sinai to the east of Abu Zenima city between latitudes 28^0 $56^/$ and 29^0 $05^/$ N and longitudes 33^0 $10^/$ and 33^0 $35^/$ E (Fig.1). The aim of this study is to characterize the distribution

of major, trace elements and radionuclides in the clastics of Abu Thora Formation.

Lithostratigraphy and geological setting:

The Paleozoic rocks have well developed exposures in Um Bogma area (Fig.1). It attains a thickness which varies from 120 to 500m, and is unconformably overlying the Precambrian basement rocks. The Abu Thora Formation reaches its maximum thickness (204m) in Thora area (type locality). Its thickness is wedging out toward both North direction within El Tih Plateau and south direction under Permo-Triassic Qaseib Formation at G. Abu Alaqa and G. Abu Gharagid. In some localities a basaltic

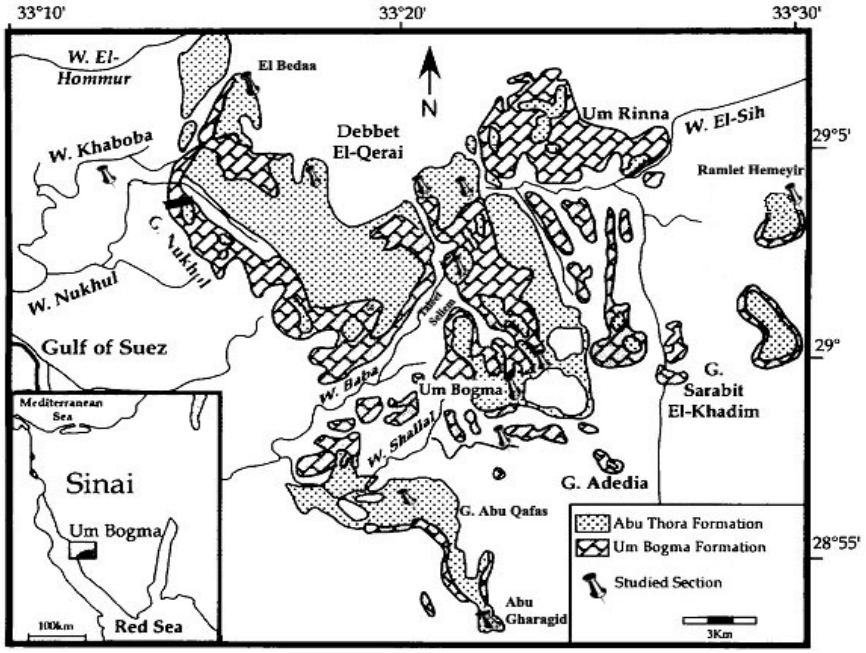

Fig. (1): Geological map of the studied area (modified after Kora and Jux, 1986).

sill (40m thick) of Late Triassic to Early Jurassic age (Weissbord, 1969, Moussa, 1987) overlies Abu Thora Formation e.g. at G. Hemeyir, G. El Allouga, G. El Farsh El Azraq and at G. Abu Qafas (Fig.2). The sandstones at the contact with the basaltic sill are metamorphosed to hard quartzite. Abu Thora Formation conformably overlies the dolostone of Um Bogma Formation and can easily be identified due to the sharp contact between the sandstones and the dolomite of Um Bogma Formation. At some localities, the contact is difficult to recognize due to laterization processes and absence of the upper dolomitic member of Um Bogma Formation. This contact is marked by highly ferruginous silty shale with manganese nodules due to latertization and thickness reduction of Um Bogma carbonates as existing at G. Hemeyir, W. El Kharig, Taleet Seliem and G. Um Bogma.

The thickness of Abu Thora Formation varies widely within the basin of deposition. It varies from 25m to 204m. The largest thickness exists at the type locality Thora area in the northwest peripheries and its vicinities at G. Hazbar and El Khaboba localities. It reaches up to 102m in the northeast direction at G. Hemeyir (Fig. 2). The thickness is reduced to 50m in the south direction at G. Abu Qafas and G. Abu Gharagid. Where it varies in the depocenter of the basin from 90m at G. Um Bogma to 25m at W. El Garf at the northern peripheries of the basin. This variation

may reflect to the uneven paleotopographic surface of the older rock units.

Abu Thora Formation is generally composed of yellowish to pinkish white sandstones intercalated by varicolored siltstone and mudstone. These mudstones grade laterally into carbonaceous shale with intercalated coal seams in some parts. The upper parts are almost snow white in color and friable (exploited as glass sand). Thin sandy conglomerate lens and gravelly layers are interbedded. Plant fossils including Lepidodendron and Sigillaria prints (Soliman and Abu El-Fetouh, 1969) are recorded in the grey carbonaceous silty facies. The relative abundance of sandstone, siltstone and mudstone within Abu Thora Formation show great variations from one place to another (Fig.2). Three main lithofacies could be distinguished from base to top; ferruginous and dirty white sandstone lithofacies; varicolored siltstone and shale lithofacies; milky white sandstone lithofacies (Abd El Halim, 2011).

METHODOLOGY

The present work was accomplished through field and laboratory studies. Forty one samples representing the different rock types (sandstone, siltstone and shale) were chemically analyzed for their major and some trace elements. The samples were discriminated as; white and ferruginous sandstones (14), varicolored siltstones (14), shale and claystones (13). The representative samples were collected along a number of lithostratigraphic sections (14 sections). These sections are

well distributed along the studied basin (Fig.1). These sections are at G. Alluoga, G.Um Bogma, G. El Farsh El Azraq, El Dabbabat, G. Hazbar, Taleet Seliem, El Hewash, Ras Nukhul, G. Hemeyir, W. El Bedaa, G. Abu Qafas, El Khaboba, El Garf and G. Abu Gharagid.

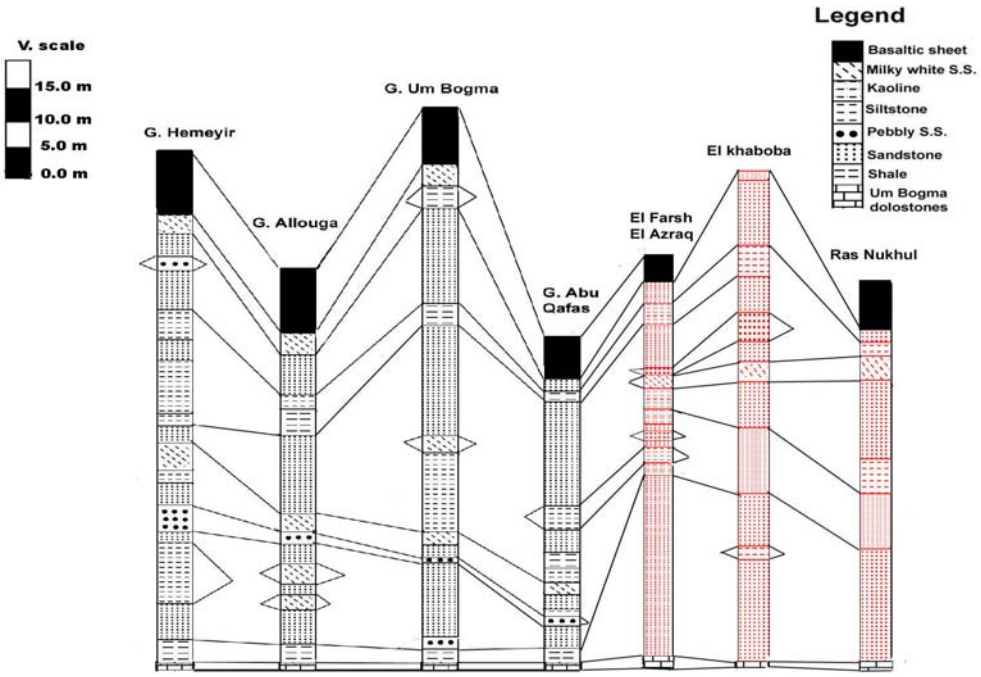

Fig. (2): Lithostatigraphic logs of Abu Thora Formation in selected localities of the study area.

The petrographic investigation of 45 samples representing the studied formation was performed on the collected intercalated sandstone samples from the studied successions. The sandstones thin sections were point-counted using the Gazzi - dickinson method (Ingersoll et al., 1984) by point counting (200-300 points per thin section). The results of the modal analyses are summarized in figs. 5(A&B).

The chemical analyses of major elements were achieved using conventional wet techniques (Shapiro and Brannock, 1962) and instrumental analysis, flame photometry, color spectrometry and some of trace elements were detected using the x-ray fluorescence technique (XRF). Mineral grain separation using heavy liquids (Bromoform, sp. Gr. 2.85) and magnetic fractionation for pure mineral separation for mineralogical investigation using the Frantz isodynamic separator. Picking of mineral grains using the optical microscope and identification of the mineral grains by X-ray diffraction analysis were carried out. Laboratory γ-ray spectrometric technique is used for the radiometric analysis of the forty-one samples for the determination of eU, eTh, Ra and K. The same samples were analyzed for chemical uranium by using the spectrophotometer colorimetry techniques.

Petrography:

The petrographic investigation shows that these sandstones framework consists mainly of quartz and, in minor amounts, feldspars, rock fragments and white micas. Several accessory minerals, such as zircon, sphene, rutile, apatite and monazite are also identified. Detrital constituents are floating or exhibit punctual tangential (Fig.3a), concavo-convex contacts (Fig.3b). The intergranular spaces are filled with a very fine grained matrix consisting mainly of kaolinite and subordinately of illite as shown by XRD data (Fig.4). Cements are chiefly of ferruginous and calcareous nature. These textural features evidence low compactation and high primary porosity. Monocrystalline quartz with straight extinction predominates over other quartz types such as monocrystalline

quartz with undulose extinction and polycrystalline quartz grains (Fig.3a). Feldspars are frequently weathered at different degrees. The rock fragments vary from altered granitic fragments, siliceous of cherty composition, argillaceous and calcareous rock fragments. These rock fragments are moderately sorted and some of them appear as opaque grains. White mica crystals are randomly distributed, occasionally millimetric in size, deformed and display common fractures. Mica is sometimes partially or almost completely altered to kaolinite. Modal abundances of quartz, feldspar and rock fragments show that the sandstones have quartz arenite (quartz grains ranging from 80-93% of the total framework components)(Figs.3c&5A), sublithic and lithic arenite (Fig.3d)(quartz grains; 64%-69%) compositions (Folk, 1968)(Fig. 5A). In order to identify the provenance of quartz grains, data have been plotted in a diamond-shaped diagram (Basu et al., 1975)(Fig. 5B). Most of sandstones plotted in the field corresponding to plutonic rocks with a few samples were in low-grade metamorphic field. So the mixed provenance was suggested. The siltstones and claystones consist mainly of clays and quartz. These fine-sized rocks have abundant Fe oxides, Ti oxides, Fe–Ti oxides, and zircons (Fig.3d). Most of these accessory phases are under few millimetres in size. The cement materials vary from iron oxides, dolomites, and silica overgrowth. The iron oxides are the most dominant and they are hematitic in composition as detected by SEM investigation.

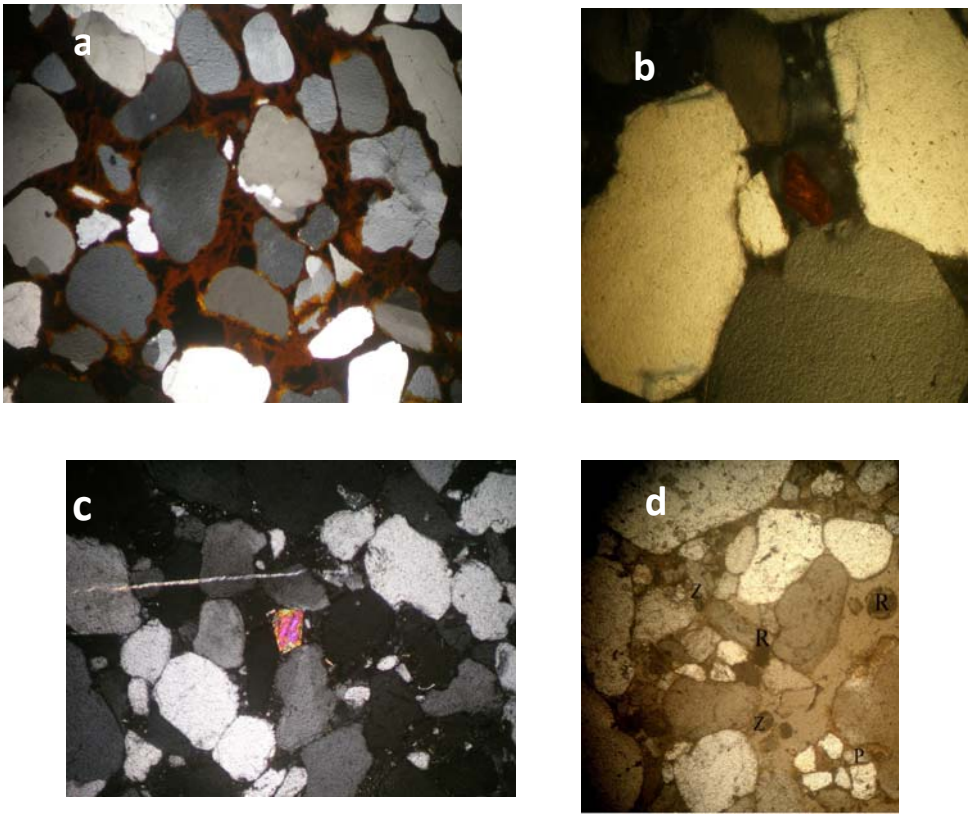

Fig.(3): (a) Quartz arenites lithofacies shows open texture composed of mono- and poly-crystalline quartz grains, cemented and floated in iron oxides mainly hematitic materials. The quartz grains showing straight to sutured contacts (C.N., X=20).

(b) Quartz arenite lithofacies of interlocked rounded to subrounded coarse monocrystalline quartz grains showing straight to concavo-convex contacts. The framework contains interspaces rutile grain. (C.N., X=40).

© Quartz arenite lithofacies showing quartz overgrowth cements. The demarcation lines showing clay minerals and silica overgrowth. The matrix contains intergranular subangular epidote grains (C.N., X=20). (d) Sublithic arenite lithofacies showing mosaic interlocking of monocrystalline quartz grains in straight to concavo-convex contacts. The demarcation lines showing iron oxides and clay minerals. The subrounded pebbly sand grains showing syntaxial contacts. The matrix contains well rounded heavy minerals as zircon (Z), rutile (R) and apatite (P) which suggest the plutonic source rocks. (P.P.L., X=20).

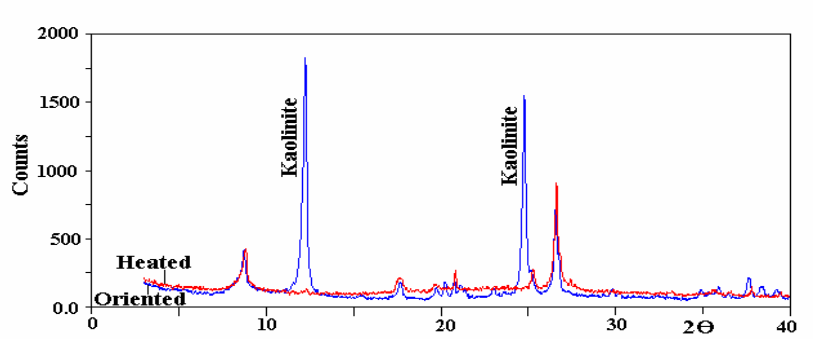

Fig. (4): X-ray diffractograms of oriented and heated clay minerals sample.

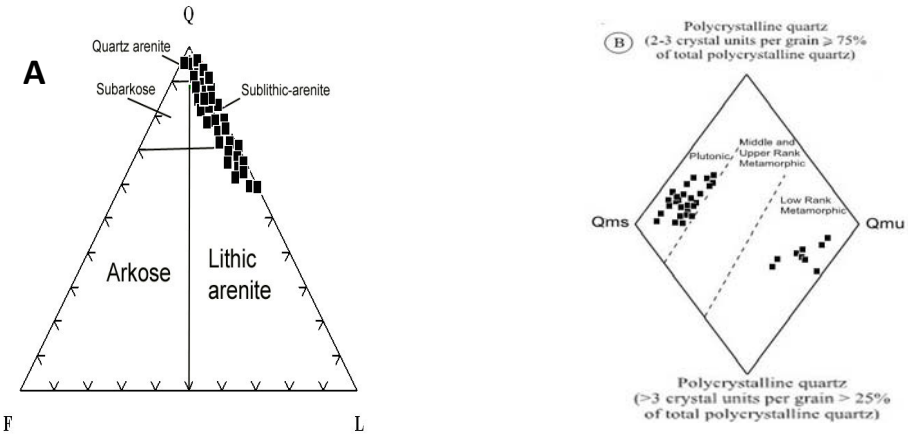

Fig.5: (A) Overall composition of sandstones of Abu Thora Fm.; classification scheme of Folk (1968) is superimposed. Q: total quartz; F: feldspar; L: rock fragments.

(B): Quartz grain varieties in sandstones plotted on diagram of Basu et al. (1975). A sample is plotted in the lower triangle if 25% or more of the polycrystalline quartz contains more than three crystallites per grain and in the upper triangle otherwise. Qms: monocrystalline quartz with straight extinction; Qmu: monocrystalline quartz with undulose extinct

Geochemistry

Forty one samples representing sandstones (14 samples), siltstones (14 samples) and shale and claystones (13 samples) were analyzed for major

and some trace elements. The minimum, maximum and the average concentrations of major and trace elements are present in table (1).

Distribution and abundance of major oxides and trace elements:

The lithofacies of Abu Thora Formation show a wide span range in its chemical composition as detected from the chemical analyses data of the studied samples (41 samples). The maximum concentration of silica (91.75%) was in the milky white sandstones lithofacies at Ras Nukhul, Bedaa, and El Khaboba localities. Such high silica content is attributed to the detrital quartz grains. While the lowest silica contents were recorded in the mineralized claystones of Taleet Seliem locality (11.6%). These mineralized claystones have the maximum contents in Al_2O_3, MgO, CaO, P_2O_5, Ni and Ga (Table 1). While the varicoloured siltstones at G. Alluoga have the maximum contents in Y and Co. The increasing of Al_2O_3 and decreasing in silica contents are attributed to breakdown of feldspars and mobilization of silica resulted from the alteration processes of the main framework components in the studied clastics. The high content of MgO in the studied sandstones is attributed to mobilization of MgO from the underlying dolostones of Um Bogma Formation which are precipitated as magnesite and hydromagnesite (Shata, 2006). These alteration processes led to liberation of magnesium and its re-precipitation in the overlying clastics as cement materials (Petrographically detected as dolomite).

The shale at G. Um Bogma has the maximum content in Fe_2O_3, P_2O_5, V and Ni content. While the grey siltstones and black shales of G. Abu Gharagid and Ras Nukhul localities have the higher content in Na_2O

(3.25%), Nb (169 ppm), Cu (292ppm) and Zr (3592 ppm) contents. Mean Zr contents for siltstones and shales (835.4 and 999.5 ppm, respectively, Table 1) are clearly higher than the same value for sandstones (747.6 ppm). This Zr distribution suggests that zircon is preferentially concentrated in siltstones. Such an assumption is supported by the Zr/Al_2O_3 ratios, clearly higher in sandstones and siltstones than in shales (265.1, 101.9 and 78.1 respectively). These values display the preferential concentration of zircon versus clay minerals in the coarser grained clastic rocks. This can be confirmed from the maximum Y content which was recorded in G. Alluoga varicoloured siltstones.

The maximum contents of Co, Zn and Sr are recorded in Bedaa ferruginous sandstones. Co has a wide range of variation as it varies from 2 to 151 ppm with an average of 18.7 ppm, with a storm sample reach up to 5462 ppm and Zn reaches up to 3433ppm in El Bedaa ferruginous sandstones. The varicoloured claystones and siltstones show slight enrichment in Co especially at G. Allouga (151ppm) and G. Hemeyir (76ppm). Ni has a maximum concentration in Taleet Seliem claystones (634ppm), W. El Garf varicolored siltstones (122ppm) and G. Hemeyir ferruginous sandstones (99ppm). While the TiO_2 and Cr maximum contents are recorded in W. El Garf red violet siltstones. This attributed to the mobility of Cr during weathering process and may be incorporated with Ti in black mafic rock fragments and phyillosilicate minerals. Generally K_2O and P_2O_5 are depleted in the studied sandstones. The maximum K_2O content was recorded in G. Um Bogma shale. While the maximum P_2O_5 content was recorded in Taleet Seliem ferruginous sandstones.

The milky white sandstones are depleted in V, Cu, Co and Ni especially at G. Allouga, Ras Nukhul, G. Hazbar, El Bedaa and W. El Dabbabat localities. While the maximum Ba concentration was recorded in El Dabbabat kaolinite lenses. The maximum Pb concentration (1232 ppm) was recorded in G. Hazbar black carbonaceous shale. This is attributed to the dominance of galena mineral grains (as detected from SEM investigation) and its concentration may be of radiogenic origin.

Generally the most mineralized lithofacies in Abu Thora Fm. are the varicoloured siltstones, carbonaceous grey and black shales and ferruginous sandstones. While the milky white sandstones is the non-mineralized lithofacies with the exception of its higher silica content (glass sand resource in southwest Sinai).

Upper Continental Crust (UCC) normalization of major and trace elements:

The studied sandstones, siltstones and shales are normalized to (UCC) upper continental crust of Taylor and McLennan (1985). The studied sandstones and siltstones are nearly enriched in SiO_2 reflecting their high detrital quartz content, while shales are depleted in silica (Fig. 6). These three facies are depleted in Al_2O_3, Na_2O, K_2O and Cr. The sandstones lithofacies are depleted in TiO_2, Fe_2O_3, CaO and MgO in comparison with their concentration in UCC. The studied sandstones, siltstones and shales are enriched in Co, Ni, Zr, V, Sr, Nb and U in comparison with UCC, while, they are depleted in Rb and Ba. The sandstones are depleted in Th in comparison with UCC (Fig.6), while it is enriched in siltstones and shales. The intensive weathering in the source

area is shown not only by the depletion in the elements selectively leachedfrom weathering profiles, such as Na, Ca and Sr (Nesbitt et al., 1980; Wronkiewicz and Condie, 1987), but also in the relatively large cations, such as K, Rb and Ba. These cations are usually fixed on clays such as kaolinite, which shows a low cation exchange capacity, i.e., a lower fixation control of these elements.

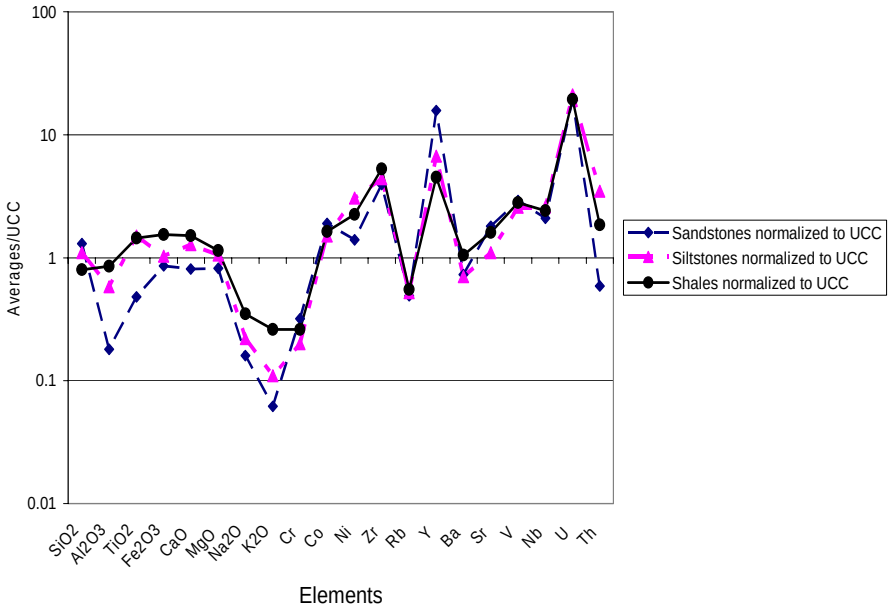

Fig. (6): Upper Continental Crust normalized major and trace elements in sandstones, siltstones and shales contents in Abu Thora Formation.

Lithology	Sandstones			Siltstones			Shales		
elements	Min.	Max.	Average	Min.	Max.	Average	Min.	Max.	Average
SiO_2	33.28	91.75	84.36	39	90.25	69.97	11.58	72.16	52.20
Al_2O_3	1.29	8.01	2.82	1.01	15.07	8.20	1.11	21.2	12.79
TiO_2	0.03	0.57	0.24	0.09	1.62	0.75	0.09	1.31	0.72
Fe_2O_3	0.39	43	4.28	0.79	19.17	5.13	2.39	22.37	7.68
CaO	1.4	5.6	3.40	1.4	16	5.34	1.4	29.4	6.30
MgO	1	5	1.79	1.0	6.0	2.29	1	11	2.50
Na_2O	0.11	1.85	0.62	0.16	3.25	0.85	0.57	2.7	1.37
K_2O	U.L.D.	0.82	0.21	0.11	1.18	0.38	0.25	2.01	0.89
P_2O_5	U.L.D.	0.33	0.08	0.009	0.22	0.10	0.02	0.23	0.09
L.O.I	0.31	3.8	1.23	0.5	11.9	4.36	1.92	13.54	8.57
ICV	0.75	11.06	3.88	0.49	8.28	2.65	0.6	45.12	5.28
Cr	U.L.D.	18	11.29	U.L.D.	20	6.90	U.L.D	89	8.91
Co	U.L.D.	151	18.7	U.L.D.	62	11.46	2	76	16.33
Ni	4	116	27.93	4	634	61.07	8	122	45.08
Cu	11	261	84.29	11	292	70.79	12	155	83.42
Zn	21	1618	234.07	23	3433	374.07	32	2231	394.67
Zr	47	1716	747.64	33	3592	835.36	51	2032	999.50
Rb	5	175	55.36	13	174	58.00	5	186	61.92
Y	U.L.D.	838	344.17	U.L.D.	544	147.11	U.L.D	222	99.27
Ba	34	969	401.93	62	1009	379.07	51	1610	579.42

Pb	**5**	**654**	**126.86**	**5**	**436**	**123.86**	**13**	**1232**	**188.42**
Sr	**39**	**3501**	**629.93**	**23**	**1269**	**384.36**	**47**	**1644**	**559.58**
Ga	**U.L.D.**	**58**	**10.8**	**U.L.D.**	**63**	**34.00**	**U.L.D**	**42**	**17.38**
V	**2**	**499**	**174.79**	**2**	**476**	**154.29**	**8**	**361**	**168.50**
Nb	**U.L.D.**	**113**	**52.6**	**U.L.D.**	**169**	**64.90**	**U.L.D**	**98**	**60.44**

Table (1): Minimum, maximum and average concentrations of major and some trace elements in Abu Thora Formation.

Correlation coefficients between major and trace elements

The following geochemical relationships can be deduced from the obtained correlation matrix of the major and trace elements (Table 2):

i. Silica (SiO_2) is negatively correlated with each of K_2O (r = -0.72), Al_2O_3 (r = -0.69), Na_2O (r = -0.58), Fe_2O_3 (r = -0.56), CaO (r = -0.50), MgO (r = -0.43), V (r = -0.70), Sr (r = -0.69), Nb (r = -0.41), Zn (r = -0.57), Cu (r = -0.53), Rb (r = -0.52), Co (r =-0.41) and Zr (r =-0.26). This can be explained that silica is the composition of the main framework components of the studied sandstones (mainly quartz and subordinately feldspars, mica and sphene). These components are diluted with the diagenetic, alteration and cement materials. This can be confirmed with the positive correlation between Al_2O_3 and each of K_2O (r = 0.68), Na_2O (r = 0.51), TiO_2 (r = 0.36), V (r = 0.67), Cu (r = 0.66), Rb (r = 0.60), Nb (r = 0.57), Ga (r = 0.56), Co (r = 0.53) and Zr (r = 0.50). On the other hand, this indicates that some trace elements are

adsorbed and fixed on clay minerals and iron oxides. This is deduced from the positive correlation between Fe_2O_3 and TiO_2 (r = 0.36), K_2O (r = 0.58), P_2O_5 (r = 0.45), Y (r = 0.53) and V (r = 0.42). The previous correlations suggest that titanium is concentrated in both phyllosilicates and other minerals such as black mafic rock fragments, silicates such as sphene and oxides such as ilmenite and rutile.

ii. The positive correlation between CaO and each of MgO (r = 0.85), Zn (r = 0.45), Th (r = 0.37) and U (r = 0.36) as well as the positive correlation between MgO and Zn (r = 0.46), show that the origin of uranium and other mobile elements (e.g. Zn, Co, V) are from the underlying mineralized dolostones of Um Bogma Formation and are precipitated by upwelling of groundwater in the studied sandstones. This can be confirmed by the positive correlation between Na_2O and each of K_2O (r = 0.55), Sr (r = 0.53), Co (r = 0.49), V (r = 0.44), L.O.I (r = 0.41), Cu (r = 0.41) and Rb (r = 0.35). These correlations are attributed to the dominance of NaCl groundwater type in the study area (Shata, 1997) and also explain the positive correlation between Ni and each of Zn (r = 0.88) and Cu (r = 0.34).

iii. The positive correlation between P_2O_5 and each of Y (r = 0.36), V (r = 0.28) and Nb (r = 0.25) is attributed to the presence of tiny monazite grains (as deduced from petrographic investigation).

iv. The positive correction between L.O.I. and each of V (r = 0.82) and Zn (r = 0.40) referred to the important source of these elements is related to the newly formed clays in the shales and siltstones that originated from the weathered basement. This confirmed with the

positive correction between Al_2O_3 with each of V(r = 0.67) and Zn (r = 0.42).

v. The positive correlation between Pb and each of Th (r=0.36) confirm the radiogenic origin of the lead content (Chiaradia and Fontbote, 2001). This radioactive series is recognized by the strong positive correlation between U and Th (r = 0.61).

Table (**2**) Correlation matrix of the studied Abu Thora Formation.

	SiO2	AL2O3	Fe2O3	TiO2	CaO	MgO	Na2O	K2O	P2O5	L.O.I	Cr	Co	Ni	Cu	Zn	Zr	Rb	Y	Ba	Pb	Sr	Ga	V	Nb	U	Th
SiO2	1																									
Al 2O3	-0.69	1																								
Fe2O3	0.56	0.20	1																							
TiO2	-0.29	0.36	0.36	1.00																						
CaO	-0.50	0.10	0.10	-0.05	1.00																					
MgO	0.43	-0.11	0.00	-0.15	0.95	1.00																				
Na2O	-0.58	0.51	0.21	-0.07	0.01	0.08	1.00																			
K2O	-0.72	0.68	0.58	0.40	0.05	0.11	0.55	1.00																		
P2O5	-0.25	0.13	0.45	0.27	0.10	0.08	0.29	0.35	1.00																	
L.O.I	0.78	0.61	0.34	0.36	0.37	0.27	0.41	0.60	0.14	1.00																
Cr	0.18	-0.24	0.05	0.19	0.04	-0.07	-0.26	-0.29	-0.06	-0.20	1.00															
Co	-0.41	0.53	-0.03	-0.19	-0.04	0.05	0.49	0.29	0.06	-0.05	-0.08	1.00														
Ni	-0.39	0.41	0.17	0.05	0.19	0.20	0.17	0.28	-0.05	0.37	-0.15	0.08	1.00													
Cu	-0.53	0.66	0.31	0.44	0.02	0.04	0.41	0.50	0.25	0.53	-0.43	0.18	0.34	1.00												
Zn	-0.57	0.42	0.13	-0.04	0.45	0.46	0.25	0.30	-0.04	0.40	-0.16	0.32	0.88	0.26	1.00											
Zr	-0.26	0.50	0.09	0.33	-0.09	-0.11	0.29	0.19	0.10	0.36	0.34	0.00	0.08	0.74	-0.03	1.00										
Rb	-0.52	0.60	0.34	0.37	-0.09	-0.16	0.36	0.64	0.27	0.74	-0.35	-0.05	0.11	0.47	0.01	0.46	1.00									
Y	-0.38	0.38	0.53	0.40	-0.11	-0.14	0.21	0.42	0.36	0.44	-0.29	-0.08	0.20	0.76	0.07	0.63	0.47	1.00								
Ba	-0.41	0.58	0.25	0.52	0.03	0.13	0.21	0.43	0.18	0.54	-0.28	-0.10	0.08	0.69	-0.05	0.71	0.67	0.59	1.00							
Pb	-0.25	0.29	0.18	0.33	0.11	-0.09	0.03	0.38	0.11	0.32	-0.20	-0.07	0.22	0.26	0.15	0.10	0.45	0.13	0.26	1.00						
Sr	-0.69	0.75	0.18	0.06	0.07	0.08	0.53	0.55	0.20	0.46	0.33	0.73	0.14	0.45	0.31	0.29	0.57	0.20	0.31	0.19	1.00					
Ga	-0.46	0.56	0.20	0.41	0.04	-0.07	0.30	0.48	0.18	0.65	0.18	0.12	0.03	0.43	0.05	0.48	0.78	0.34	0.65	0.50	0.39	1.00				
V	-0.70	0.67	0.42	0.51	0.14	0.05	0.44	0.71	0.28	0.82	-0.44	-0.05	0.25	0.76	0.19	0.62	0.80	0.68	0.79	0.40	0.47	0.77	1.00			
Nb	0.41	0.57	0.26	0.47	-0.13	-0.16	0.40	0.46	0.25	0.56	-0.35	-0.10	0.08	0.61	-0.07	0.84	0.69	0.71	0.83	0.18	0.33	0.68	0.85	1.00		
U	-0.03	-0.18	0.04	0.03	0.37	0.32	-0.06	-0.22	-0.13	0.07	0.14	-0.29	0.08	-0.07	0.09	0.09	0.11	0.15	0.05	0.04	-0.25	-0.05	-0.01	0.03	1.00	
Th	-0.25	0.05	0.25	0.36	0.36	0.17	0.04	0.05	0.13	0.19	0.38	-0.09	0.13	0.02	0.16	0.00	0.08	-0.09	0.04	0.36	0.04	0.11	0.05	0.02	0.61	1.00

Provenance:

Different discrimination diagrams were employed (Bahatia, 1983, Roser and Korsch, 1986 and 1988) in order to infer the provenance material using the major element and confirmed with the petrographic composition. In Roser and Korsch (1986) discrimination diagram (Fig.7A), exhibits that all the samples lie within the active continental margin provenance except three samples lying within the passive margin. Also Roser and Korsch (1988) discrimination diagram (Fig. 7b) shows

that Abu Thora Formation has a mixed provenance of felsic and intermediate igneous provenance. This is confirmed by the high proportion of the monocrystalline quartz grains, and absence of stretched quartz grains and polycrystalline grains with elongate crystals and relatively straight intercrystalline boundaries which suggests an absence or rarity of schistose and gneissic terrains in the source area (Dampare, 2004). Lithic fragments are mainly granitic and subordinately metamorphic parent rocks. This confirms the mixed provenance from continental margin and recycled orogen.

Inferred tectonic setting of the depositional basin:

Determination of tectonic setting of clastic sediments from major oxides chemistry began with the work of Middleton (1960), Crook (1974) and Schawb (1975) and continued with Bhatia (1983), Roser and Korsch (1986), and Kroonenberg (1994). Bhatia (1983); Bhatia and Crook (1986) proposed a classification of sedimentary basins based on simplified plate tectonic classification of continental margins and oceanic basins according to the nature of the underlying crust. Abu Thora sandstones show relative depletion of mobile oxides (e.g. CaO, Na_2O) and enrichment of immobile oxides (e.g. SiO_2, TiO_2). These geochemical conditions are consistent with active continental margin tectonic setting due to the relative tectonic stability and hence protracted weathering and high degree of recycling of sediments (Bhatia, 1983; Roser and Korsch, 1988). In (Fig.7c) most of Abu Thora samples lie in active continental margin setting. The Bhatia (1983) diagram plots the major elements of Abu Thora Formation (Fe_2O_3 + MgO% vs. Al_2O_3/SiO_2) (Fig.7c) and

(Fe_2O_3+MgO% vs. TiO_2) (Fig.7d). These diagrams show that the majority of the samples fall in the active continental margin. Some samples fall outside or adjacent to this field.

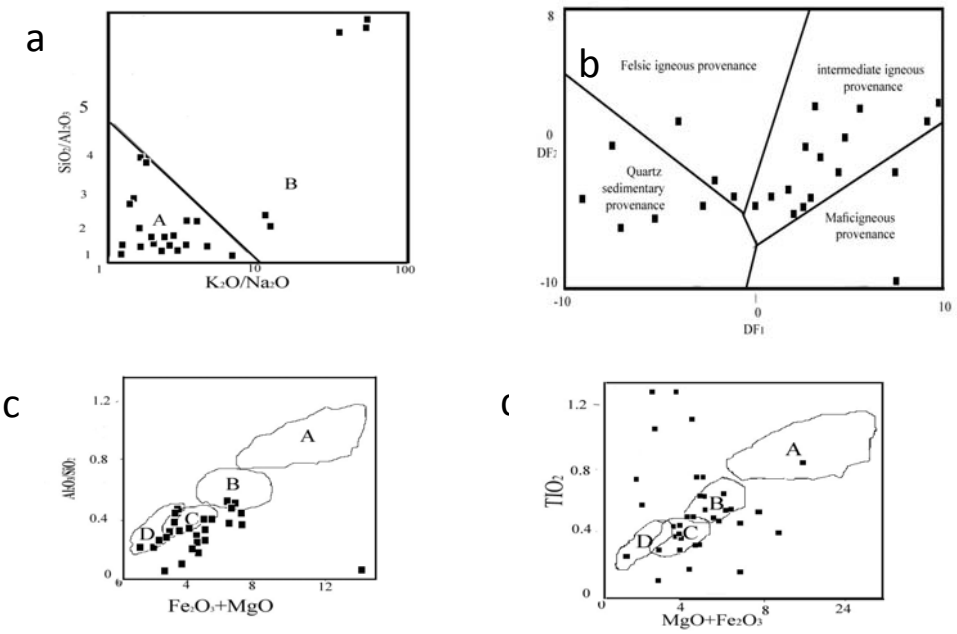

Fig. (7): **(a)** Tectonic setting discrimination diagram for clastic sediments after Roser and Korsch (1986). A= Active continental margin B= Passive margin. **(b)** Provenance diagram after Roser and Korsch, (1988) **(c)**&(d) Major element composition plots for tectonic setting discrimination of clastic sediments after Bhatia (1983)
A= Oceanic island arc margin. B= Continental island arc margin. C= Active continental margin. D= Passive continental margin.

Source area composition and weathering:

The main approach toward assessing original detrital mineralogy of the studied clastics is to use the index of compositional variability (ICV) of Cox et al., (1995); ICV= [(Fe_2O_3+K_2O+Na_2O+CaO+MgO+TiO_2)/Al_2O_3]. Since immature mudstones with a high percentage of non-clay silicate minerals will

exhibit ICV values greater than (1). This exists in tectonically active settings as first cycle of deposition (Van de Kamp and Leake, 1985). In contrast, the more mature mudstones with mostly clay minerals display lower (ICV) values that are less than (1) (Cox et al., 1995). These mudstones are formed where recycling and weathering processes dominate and may be found in some intensely weathered first cycle material deposits in tectonically active provenance. The ICV value of Abu Thora sandstones range from 0.75 to 11.06 with an average of 3.96, while ICV value of Abu Thora siltstones range from 0.49 to 8.28 with an average of 3.04, also ICV value of Abu Thora shales range from 0.60 to 14.15 with an average of 2.7, this suggesting that most samples are compositionally immature and dominated by sediments of first cycles of deposition. This result is consistent with the generally low amounts of feldspar in the sandstones of Abu Thora Formation. The chemical index of alteration (CIA; CIA = $[Al_2O_3/ (Al_2O_3+ CaO^* +Na_2O+ K_2O)] x100$) is used to infer the degree of source area weathering (Nesbitt and Young, 1982). This index can be calculated using molecular proportions, where CaO* represents the amount of CaO associated with the silicate fraction of the rock.

The calculated CIA values (ranges from 18.8 to 93.6) of Abu Thora Formation (sandstones, siltstones and shales) shows that the source area are exposed to intensive weathering. In general, the high amounts of quartz relative to feldspar and rock fragments in the sandstone facies could be related to significant chemical weathering of a granitoid source area. CIA values of the analyzed samples range from 18.8 to 93.6, with mean values of 49.6, 51.2, and 53.1 for sandstones, siltstones and

claystones, respectively. CIA values in siltstones and shales are higher than value of UCC (<50) and lower than the typical average value in shales (70–75). Therefore, the moderate CIA values suggest a significant degree of weathering of first cycle sediment, or alternatively, these recycling could have produced these interbedded claystones and siltstones. The CIA values of Abu Thora Fm. indicate that these sediments were generated from a source area strongly affected by significant chemical weathering.

Radioactivity

Radiometric characteristics of Abu Thora Formation:

The eU contents in the varicoloured siltstones reach up to 162 and 43 ppm at Taleet Seliem and W. El Kharig respectively with an average of 24.72 ppm. This lithofacies is considered the most radioactive rock unit in Abu Thora Formation. The eTh in the varicolored siltstones lithofacies reaches up to 309 ppm at El Khaboba locality with an average of 37.1 ppm. The eTh/eU ratio in this locality reaches up to 7.19 with an average of 1.91 ppm (Table 3). While the eU contents in white sandstones lithofacies reaches up to 20 ppm at W. El Bedaa. The average eU and eTh/eU ratio of the white sandstones is 6 and 1.5 ppm respectively. While the eU contents in ferruginous sandstones ranges from 2 ppm at G. El Farsh El Azraq locality to 31 ppm at G. Abu Gharagid with an average of 13.2 ppm. In this lithofacies,eTh reaches up to 25 ppm at G. Abu Alaqa locality with an average of 10.4 ppm. The radium content reaches up to 53 ppm at G. El Farsh El Azraq. This indicates that

U is recently leached out from the ferruginous sandstones in the base of Abu Thora Formation. The average eTh/eU ratio is 1.13 in the conglomeratic sandstones laminae this attributed to the presence of Th-bearing detrital heavy minerals. The eU contents in black carbonaceous shales range from 4ppm at G. Abu Qafas to 21ppm at Ras Nukhul locality with an average of 9.72 ppm. While Ra reaches up to 17 ppm in Ras Nukhul black shales with an average of 6.61ppm. The eTh content in this lithofacies reachs up to 35 ppm at G. Abu Qafas locality with an average of 19.78 ppm. While the average eTh/eU ratio is 2.12 ppm.

Table (3): Average radionuclides concentration in different facies of Abu Thora Formation.

S. No.	Lithofacies	eU	eTh	Ra	K%	eTh/eU
1	Ferruginous sandstones	13.4	10.4	16.2	0.62	0.81
2	Conglomeratic pebbly sandstones	2	2	1.2	U.L.D	1.13
3	Coal bearing black shales	9.72	19.78	6.61	0.36	2.12
4	Varicolored siltstones	24.72	37.09	18.0	0.24	1.91
5	White sandstones	6.0	2.83	1.16	0.035	1.5

Radioactive anomalies:

The radiometric and chemical analyses of uranium in the collected samples of the studied Abu Thora Formation show that there are about twenty two (22) radioactive anomalies distributed in the five lithofacies

of Abu Thora Formation. These anomalies are in the varicolored siltstones facies (7 anomalies) located at G. Abu Alaqa, G. Abu Qafas, W. El Dabbabat, G. Hazbar, W. El Garf, G. Hemeyir and G. El Farsh El Azraq localities. It contain a chemical uranium (Uc) ranges from 46 ppm to 72 ppm with an average of 58.9 ppm (Table 4). This means that the varicolored siltstones facies is enriched in U mainly at the northern sector of the depositional basin as well as at G. El Farsh El Azraq. This lithofacies is considered the most radioactive lithofacies in the studied clastics (Fig.8).

The second anomalous facies is the black carbonaceous coal-bearing shale (6 anomalies). These anomalies are located at G. Abu Gharagid, G. Abu Qafas, G. Hemeyir, G. Hazbar, Ras Nukhul and G. El Farsh El Azraq. These anomalies have Uc ranges from 48 to 70 ppm with an average of 55.8 ppm (Table.4). The anomalies are located along the southern and northern peripheries of the depositional basin. The third anomalous facies is the ferruginous sandstones and gibbsite bearing-shale exist in the base of Abu Thora Formation (5 anomalies) located at G. Abu Gharagid, Taleet Seliem, G. Hemeyir and G. Alluoga. These anomalies contain Uc ranges from 41 to 70 ppm with an average of 54.2 ppm.

The forth anomalous facies is the white sandstones contain kaolinite lenses exist at the topmost part of Abu Thora Formation (4 anomalies). These anomalous facies are located at W. El Khaboba, Taleet Seliem, G. Hazbar and W. El Hewash localities. Uc in these rock units ranges from 39 to 62 ppm with an average of 51 ppm (Table. 4). This means that the sandstones ridge extends from G. Alluoga in the south passing through

G. Hazbar and Ras Nukhul area in the north, is enriched in uranium and may be structurally controlled with NNW-SSE normal fault extending along W. Naseib. This structure line facilitates the circulation of U-bearing groundwater in this sandstone ridge.

The fifth anomalous facies is the pebbly conglomeratic sandstones which exhibit radioactive anomaly at G. Abu Qafas (50 ppm) and G. Hazbar (48 ppm) localities.

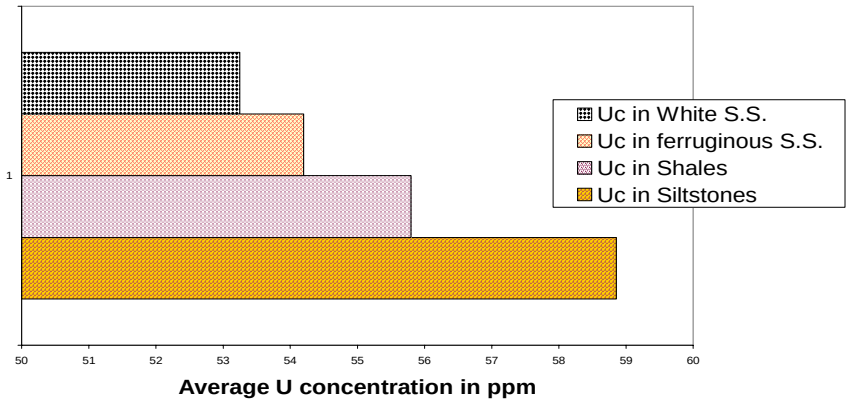

Fig.(8): Average U concentration in different lithofacies of Abu Thora Foramtion.

Radioactive disequilibrium in Abu Thora Formation:

The ability to correlate directly between radiometric measurements and the amount of Uc in the rocks or soils is wholly dependant on the status of equilibrium between U and its daughter products. This is true because the radioactivity is from those daughter products (specifically Bi-214 and Ra-226) and not U itself. The relation between the Th/U ratios and U contents in ppm (Fig.9a) shows negative correlation, which

indicates some enrichment of U relative to thorium (U was enriched during secondary processes). The ratio between the measured chemical uranium to radiometric uranium (Uc/eU; D- factor of Hansink, 1976) in the mineralized and non mineralized samples of Abu Thora Formation are given in table (4). It revealed that most of the studied samples have a ratio greater than 1. It ranges from 0.09 to 58 with an average of 12.7. The mineralized samples have a ratio up to 52. This indicates the presence of strong positive disequilibrium in the studied sediments i.e. the chemical U is higher than the radiometric U (Uc/eU > 1; positive disequilibrium) (Table 4). This means that U in these rock units has been transported recently and has not enough time for daughters to be produced. This is confirmed with the negative relationship between U and Th/U (Fig.9a) as well as the high Ra content in the studied samples. Th and U are commonly fractionated during surficial processes. This is due to the relative solubility of oxidized uranium in surficial environments, as compared to the relatively immobile Th, which is concentrated in residual materials (Wedepohl, 1978). Thus, the intensely weathered profiles display high Th/U ratios. This is consistent with the increase in mean Th/U values in siltstones and shales than sandstones lithofacies. Also, U has a strong direct relationship with Y (Fig.9b) due to the detrital mode of U occurrence in the studied clastics (mainly monazite) as detected from petrographic studies.

a

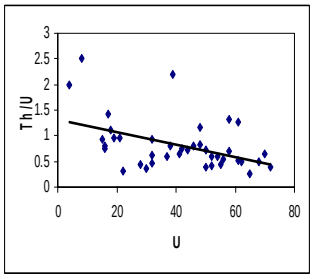

b

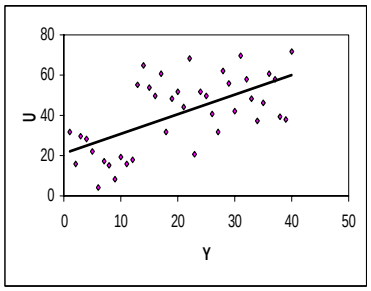

Fig (9) Relation between each of U and Th/U (a) and Y(b).

Table (4) Radiometric and chemical analyses of the radioactive anomalies in the Abu Thora Formation.

S. No.	Sample No.	eU ppm	eTh ppm	Ra ppm	eTh/eU	Uc ppm	U/eU	Lithofacies
1	Agh-1	31	25	53	0.81	52	1.6	**Black shale**
2	Kh-1	43	309	9	7.2	39	0.91	**White S.S.**
3	Tsa-1	162	11	136	0.07	50	0.31	**Siltstone**
4	AQ-1	2	35	14	17.5	46	2.2	**Siltstone**
5	Hw-7	6	10	3	1.7	72	12.0	**Siltstone**
6	Hw-1	11	17	9	1.6	62	5.6	**White S.S.**
7	Tsb-1	10	3	10	0.3	70	7.0	**Ferruginous S.S.**
8	Agh-19	9	13	5	1.4	68	7.6	**Siltstone**
9	Db-2	5	10	2	2.0	61	12.2	**Siltstone**
10	Ag-3	4	2	1	0.5	60	15.0	**Ferruginous S.S.**
11	Kh-5	10	18	6	1.8	50	5.0	**Conglomeratic S.S.**
12	HR-23	9	10	6	1.1	55	6.1	**Black shale**
13	AQ-4	1	2	1	2.0	52	52.0	**Black shale**
14	GF-1	5	11	4	2.2	61	12.2	**Siltstone**
15	HR-1	9	13	9	1.4	56	6.2	**Siltstone**

16	Tsa-6	13	13	10	1.0	58	4.5	**White S.S.**
17	Tsb-7	4	41	1	10.3	41	10.3	**Ferruginous S.S.**
18	Hz-3	1	2	1	2.0	48	48.0	**Conglomeratic S.S.**
19	Sh-13	11	20	8	1.8	48	4.4	**Black shale**
20	Sh-5	6	2	3	0.33	54	9.0	**White S.S.**
21	Hz-1	12	23	8	1.92	58	4.8	**Black shale**
22	Rkh-2	28	13	48	0.43	70	2.5	**Black shale**

Mineralogy of the radioactive lithofacies in Abu Thora Formation:

Fifteen (15) radioactive samples were subjected to different mineralogical technique. This investigation revealed the distribution of heavy minerals controlled the radioactivity in Abu Thora Formation. The identified heavy minerals assemblages consists mainly of the oxides and oxhydroxides of iron and titanium minerals such as goethite, ilmenite, hematite, leucoxene, kaolinite, zircon, sphene and copper ore mineral; rosasite.

Sphene: $CaTiSiO_5$

It is detected with XRD, SEM and petrographic investigations (Figs. 10b&c&11). It exists as prismatic, wedge shape brownish, green and grey crystals. In thin section, it occurs as four-side lozenge-shaped forms (Fig.10b). It may be the alteration of detrital ilmenite mineral (leucoxene) or directly detrital from acidic source rocks of magmatic origin**.** Relatively high amounts of Ti- oxides can be formed, during the weathering of an acidic igneous rock through the breakdown of host

species such as biotite, hornblende, etc. Thus, the immobile elements released, such as Ti, Nb and Y should be distributed between residual and new secondary minerals. These minerals could have been formed as supergenic residual minerals in humid and warm climates, and could have remained stable in conditions of lateritic weathering.

Apatite: $Ca_5 (PO_4)_3F$

It is detected in petrographic investigations. It is green, brown to dark brown lath like or wedge shaped hexagonal crystals. It observed in the interspaces and as inclusions of main framework grains of the plutonic lithic fragments.

Zircon: $ZrSiO_4$

It is detected with XRD, SEM (Fig.10d) and petrographic investigations (Fig.3d). It exists as colourless, pale pink subrounded to rounded and metamict anhedral corroded grains. It also occurs as idiomorphic bipyramidal and broken as well as rounded crystals which refer to the distant source rocks and long distance of transportation.

Kaolinite:

Kaolinite was identified in bulk and oriented sample with XRD diffraction. It detected by XRD (Figs. 4&11) and SEM investigations of the mineralized samples.

Rosasite: **$(Cu,Zn)_2(CO_3)(OH)_2$**

It is detected with XRD investigation associated with heavy fraction of G. Um Bogma varicoloured siltstones (Fig.11). It is found associated with kaolinite and zircon grains. It is common in the oxidation zone of Zn-Cu-Pb deposits associated with other copper carbonates (malachite and azurite are common in the study area). It is considered minor ore of copper.

a

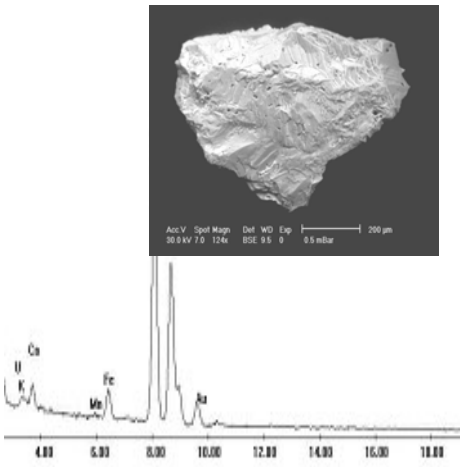

C

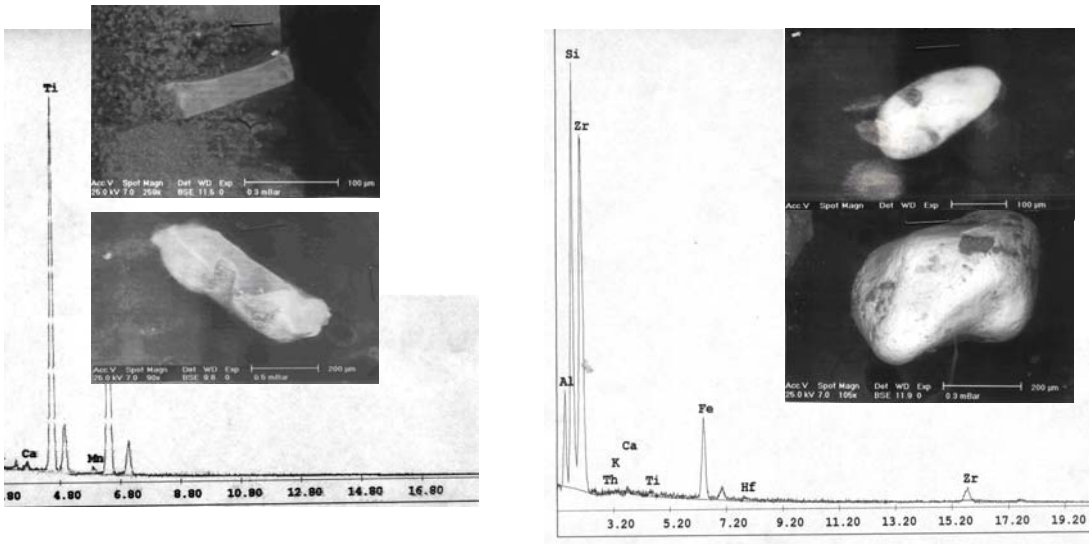

Fig. (10): a. EDX and SEM of rosasite mineral. b. Photomicrograph of quartz arenite contain interspaces sphene (S) grains (C.N., X=20). C. EDX and backscattered SEM images of sphene mineral. d. EDX and backscattered SEM images of zircon mineral.

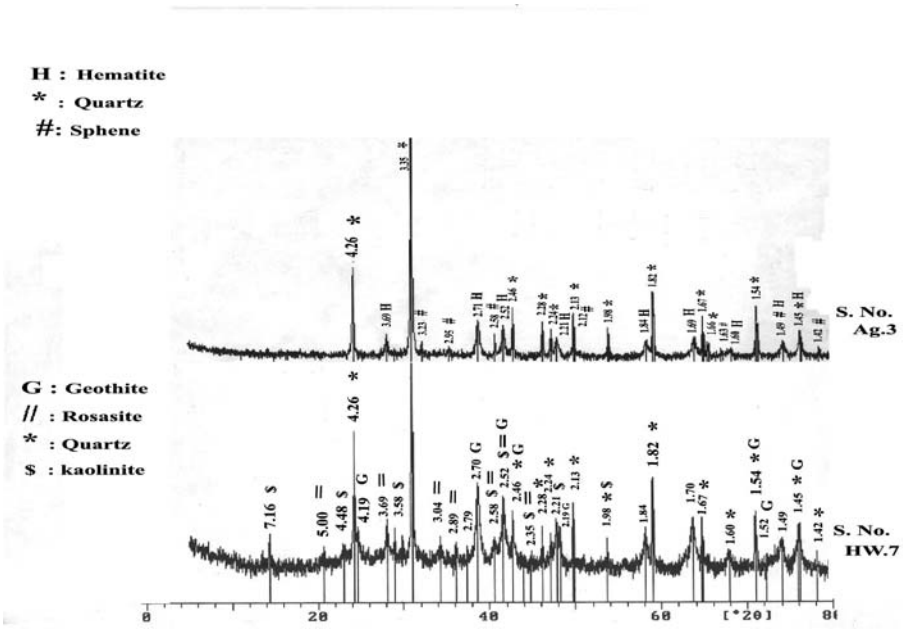

Fig. (11): X-ray diffractograms of radioactive heavy fractions of ferruginous sandstone (Ag.3) and varicoloured siltstones (HW.7) samples in Abu Thora Formation.

CONCLUSION

The Abu Thora Formation deposited in a terrestrial foreland basin in active continental margin tectonic setting. The provenance of quartz grain revealed the mixed plutonic and low grade metamorphic parent rocks. These clastics are enriched in Co, Ni, Zr, V, Sr, Nb and U in comparison with Upper Continental Crust (UCC). While, they are depleted in TiO_2, Fe_2O_3, CaO, MgO, Rb and Ba. Abu Thora Formation

shows a positive disequilibrium where the chemical U is more than the radiometric ones due to recent enrichment and mobilization from underlying source rocks. The mineralogical, geochemical, petrographic and radiometric investigations revealed that uranium concentration in Abu Thora Formation was controlled by:

i. Lithofacies control: uranium is concentrated in the siltstones and carbonaceous shale lithofacies which are enriched in iron oxides and clay minerals which have the ability of adsorbing uranium from circulating solutions.

ii. Structural control: uranium in Abu Thora Formation is associated with the occurrence of structure lines as N-S normal faults at W. El Kharig extending to Ras Nukhul and El Khaboba localities. NW-SE normal faults of W. Naseib affecting in G. Allouga and extending as a right limb to W. El Sahu graben. The fracturing accommodating the emplacement of dykes associated with the Gulf of Suez rifting.

iii. Topographic control: Those landforms are capped by basaltic sheets as at G. Allouga, G. Hemeyir, G. Um Bogma, G. Abu Qafas and G. El Farsh El Azraq localities have relatively high uranium content than the other localities which have no basaltic sheet. This basaltic cover act as aquitard with the underlying Um Bogma Formation dolostones.

iv. The detrital minerals content: The anomalous U content in Abu Thora Formation is controlled mainly to the presence of U-bearing detrital grains such as zircon, monazite, apatite and sphene.

v. Mobilization factor: Uranium and other mobile elements might have been remobilized from the Precambrian granites and underlying anomalous Um Bogma Formation. This lead to the enrichment of interbeded mudstones and siltstones which are enriched in iron oxides, clay mineral and organic matter which are the main capture of the leachable uranium from the detrital mineral grains as well as the other source rocks.

REFERENCES

Abd El- Halim, K.A. (2011): Geological and geochemical studies on Abu Thora Formation, Southwest Sinai, Egypt. M.Sc. thesis, Fac. Sci., Menoufiya Univ. 120p.

Basu, A., Young, S.W., Suttner, L.J., James, W.C., Mack, G.H.,(1975): Re-evaluation of the use of undulatory extinction and polycrystallinity in detrital quartz for provenance interpretation. J. Sediment. Petrol. 45: 873– 882.

Bhattacharyya, D.P. and Dun, L. G., (1986): Sedimentologic evidence for repeated pre-Cenozoic vertical movements along the northeast margin of the Nubian Craton. J. Afr. Earth Sci., (2): 147-153.

Bhatia, M. R. (1983): Plate tectonic and geochemical composition of sandstones. J. Geol., 91: 611-627.

Bhatia, M. R. and Crook, K. A. W. (1986): Trace elements characteristics of greywacke and tectonic setting discrimination of sedimentary basins. Contribution to Mineral. and petrol., 92: 181-193.

Blatt, H. Middleton, G. and Murry, R. (1980): Origin of sedimentary rocks. Prentice-Hall. Englewqqd Clift. N. J., 2nd ed. 782 p.

Chiaradia, M. and Fontbote, L., (2001): Radiogenic Lead signatures in Au-rich volcanic-hosted massive sulfide ores and associated volcanic rocks of the early Tertiary Macuchi Island Arc (Western Cordillera of Ecuador). Econ. Geol., 96: 1361-1378 .

Cox, R., Lowe, D. R. and cullers, R. L. (1995): The influence of sediment recycling and basement composition on evolution of mud rock chemistry in the southwestern United States. Geochim Cosmochim Acta, 59: 2919-2940.

Crook, K. A. W. (1974): and ancient Geosynclinals sedimentation. SEPM Spec. publ., 19 Lithogenesis and tectonics: the significance of compositional variation in flysch arenites (greywacke). In: Dott, R. H. and Shaver, R. H. (eds.) Modern. p. 304-310.

Dampare, S. B. (2004): Lower Proterozoic greywacke from the Birm Diamondiferous field. Ghana. J. of Science and Technology, 5: 9-18.

El- Agami, N. L. (1996): Geology and radioactive studies on the Paleozoic rock units in Sinai Peninsula, Egypt. Ph. D.Thesis. Mansoura Univ. Egypt. 302 P.

El –Aassy, i. E. Botros, N. H. Abd el Razik, A. Sherif, H. Al Moafy. A. Aita, K. El Terb, R. Al Shami, A. S. (1986): Report on the prospection and proving of some radioactive occurrences in west centeral Sinai, Egypt. Internal Report. Nuclear Material Authority (NMA), Cairo.

El –Aassy, I. E., Ahmed, F. Y., Shata, A. E. , Mohammed, G. A. , Al Shami. A. S., Gabr, M. M. and Rabboh, A. A. (2006): New resources of rare earth elements in Sinai, Egypt. 7Th inter. Conf. on Geochemistry, Fac. Sci. Alex. Univ., Alex., Egypt, 6-7 Sept. 2006; v.III: 177-184.

El Kelani. A., I. El Hag, Bakry and M. Shaira (1999): Type and stratotype section of the paleozoic in Sinai, EGSMA sp. 77, 94 p.; Cairo.

El-Sawey, S. (2008): Mineralogical studied on Magharet El Maih sandstones. W. sahu, southwestern Sinai, Egypt. Sedimentology of Egypt. 16: 161-174.

El- Shazly, E. M. Shukri, N. N. and Saleeb, G. S. (1963): Geological studies of Oleilcat, Marahil and Um Sakran Manganese- iron deposits west central Sinai, Egypt. J. geol. U. A. R. 7, 1- 127 p.

El Shazly, E. M., Abdel Hadi, M. A., El Ghawaby, M. A., El Kassas, I. A. and El Shazly, M. M. (1974): Geology of Sinai Peninsula from ERTS-1 Satellite images. Cairo Acad. Sci. Res. Tech., 20 p.

Folk, R., (1968): Petrology of Sedimentary Rocks. Hemphill's, Austin, p. 177.

Hansink, J. D. (1976): Equilibrium analysis of a sandstone roll-front uranium deposit, in Exploration for uranium ore deposits, IAEA: 683-693.

Hussein, H. A., Abdel Monem, A. A., Mahdy, M. A., El Assey, I. E. and G. A. Dabbour, (1992): On the genesis of surfical uranium occurrences in west central Sinai Egypt. Ore geol. Rev. 7: 125-135.

Ingersoll, R.V. Bullard .T. F. Ford.R.L. Grimn .J. P. Pickle. J. D. and Sares . S.W. (1984): The effect of grain size on detrital modes a test of the Gazzi- Dicknson point- counting method. J. Sed. Petrol. 54: 103-116.

Issawi, B. and Jux, U. (1982): Contributions to the stratigraphy of the Paleozoic rocks in Egypt: Geol. Surv. Egypt: 64- 28.

Kora, M. (1984): The Paleozoic outcrops of Um Bogma area Sinai, ph. D.Thesis, Mansoura Univ., Egypt. 280 p.

Kora, m. and Jux, U. (1986): On the Early Carboniferous macrofauna from Um Bogma Formation, Sinai, N. Jb.Geol. Palaont. Mh., 2: 85-95.

Kostandi, A. B. (1959): Facies maps for the study of Paleozoic and Mesozoic sedimentary basins of the Egyptian Region. 1st Arab Petrol. Congr, Cairo, 2: 54-62.

Kroonenberg, S. B. (1994): Effect of provenance, sorting and weathering on the geochemistry of fluvial sands from different tectonic and climatic environments. Procceding 29 Th Int. geol. Congr, part a: 69-81.

Mclennan, S. M. (1985): Rare earth elements in sedimentary rocks influence of provenance of mineralogy, 21: 169-196.

Middleton, G. V. (1960): Chemical composition of sandstone. Geol. Soc. Amer. Bull., 71: 1011-1026.

Moussa, H. E. (1987): Geologic studied and genetic correlation of basaltic rocks in west central Sinai. Ph.D. Thesis, Fac. Sci, Ain Shams Univ., Egypt. 308 p.

Nesbitt, H. W., and Young, G. M. (1982): Early proterozoic climate and plate motions inferred from major elements chemistry of lutites. Nature, 299: 715-717.

Nesbitt, H.W., Markovics, G., Price, R.C., (1980): Chemical processes affecting alkalines and alkaline earths during continental weathering. Geochim. Cosmochim. Acta 44: 1659–1666.

Omara and Schult, (1965): A lower carboniferous Microflora from Southwest Sinai. Paleontegraphic B. 117, Abt, B. Egypt.: 47- 58.

Pettijhon, F. J. Petter, P. E., and Siever, R. (1972): Sand and sandstone springer verlog, New York, 618 p.

Roser, B. p. and Korsch, R. J. (1986): Determination of tectonic setting of sandstone-mudstone suites using SiO_2 content and K_2O/Na_2O ratio. J. Geol., 94: 635-650.

Roser, B. p. and Korsch, R. J. (1988): Provenance signatures of sandstones- mudstones suites determined discrimination function analysis of major elements data. Chemical Geol. 67: 119- 139.

Said. R. (1971): Explanatory Notes to Accompany the Geological Map of Egypt. Geol. Surv. Egypt, Cairo, 56: 123p.

Schawb, F. L. (1975): Framework mineralogy and chemical composition of continental margin-type sandstone. Geol. 3: 487-490.

Shapiro. L. and Brannnock, W. W. (1962): Rapid analysis of silicate, carbonate and phosphate rocks. U.S. Geol. Surv. Bull, 1114-A.

Shata, A. E. (1997): Geological, hydrogeological, and geochemical characteristics affecting the behavior of uranium in some rock exposures, southern Sinai, Egypt. Mansoura Univ. M.Sc. Thesis, 186 p.

Shata, A. E. (2002): Geological and geochemical studies on uranium and thorium of selected basal sandstones exposures in southern Sinai, Egypt. Mansoura Univ. D. Ph. Thesis, 189 p.

Shata, A. E. (2006): Role of epigenetic processes in the enrichement of mineralized dolostones of Um Bogma Formation, Southwestern Sinai. Sed. of Egypt. 14: 219-242.

Soliman, S. M. and Abu El- Fetouh, M. (1969): Petrology of the Carboniferous Sandstone in west central Sinai. J. Geol. Univ. A. R., 13/2: 61-143.

Van de Kamp, P. C. B.E. Leake and A. Senior, (1976): The petrography and geochemistry of some Californian arkoses with application to identifying gneisses of sedimentary origin. J. Geol. 84: 195-212.

Taylor, S.R., McLennan, S.M., (1985): The Continental Crust: Its Composition and Evolution. Blackwell, Oxford, p. 312.

Wedepohl, K.H., (1978): Handbook of Geochemistry. Sect. II, 92-G1. Springer, Berlin.

Weissbrod, T. (1969): The Paleozoic outcrops in south Sinai and their correlation with those of southern Israel, in the Paleozoic of Israel, and the adjacent countries. Geol. Surv. Israel. Bull. No. 47, pt.2: 2, 32 p.

Weissbrod, T. (1980): The Paleozoic of Israel and adjacent countries (lithostratigraphical study) Ph. D. Thesis, Hebrew Univ., Jerusalem, 275 P. (with English Abstract).

Wronkiewicz, D.J., Condie, K.C., (1987): Geochemistry of Archean shales from the Witwatersrand Supergroup, South Africa: source-area weathering and provenance. Geochim. Cosmochim. Acta. 51: 2401–2416.